

Cocktail effect on superconductivity in hexagonal high-entropy alloys

Bin Liu^{1*}, Wuzhang Yang^{2,3,4}, Guang-Han Cao⁵, and Zhi Ren^{2,3†}

¹*Faculty of Materials Science and Engineering, Kunming University of Science and Technology, Kunming, Yunnan 650000, PR China*

²*School of Science, Westlake University, 18 Shilongshan Road, Hangzhou 310024, Zhejiang Province, PR China*

³*Institute of Natural Sciences, Westlake Institute for Advanced Study, 18 Shilongshan Road, Hangzhou 310024, Zhejiang Province, PR China*

⁴*Department of Physics, Fudan University, Shanghai 200433, PR China and*

⁵*School of Physics, Zhejiang University, Hangzhou 310058, PR China*
(Dated: November 12, 2024)

We report the study of the cocktail effect on superconductivity in high-entropy alloys (HEAs), using hexagonal close-packed HEAs as a prototype system. Compared with the compositional averages of the constituent elements, the superconducting transition temperature T_c is enhanced by from a factor of ~ 2 to over one order of magnitude. This T_c enhancement correlates with the reduction in the Debye temperature, underlining the importance of phonon softening in triggering the cocktail effect. Furthermore, we show that the T_c in these HEAs is governed by the average phonon frequency and electron-phonon coupling strength, the latter of which scales linearly with the inverse HEA molecular weight and is progressively weakened with increasing mixing entropy. Our study paves the way toward quantitative understanding of the superconductivity in HEAs.

1. INTRODUCTION

Over the past decade, a new class of compositionally complex alloys developed based on the entropy concept, the high-entropy alloys (HEAs), have attracted much attention [1–4]. These emerging alloys are made up of four or more principle elements with equimolar or nearly equimolar ratios. This chemical complexity leads to enhanced mixing entropy, which overcomes the enthalpies of compound formation. As a consequence, HEAs exist in a single solid-solution phase and are often regarded as metallic glasses on an ordered lattice. Compared with traditional alloys based on one or two principle elements, HEAs often exhibit superior mechanical and physical properties, such as high hardness [5], high thermal stability [6], excellent corrosion resistance [7], complex magnetism [8], and robust superconductivity against disorder [9].

In principle, HEAs are anticipated to possess four core effects, including a high-entropy effect for thermodynamics, a lattice distortion effect for structure, a sluggish diffusion effect for kinetics, and a cocktail effect for properties [2–4]. Especially, the cocktail effect means that the elements that make up the HEAs work in synergy with each other to enable better performance than the compositional average. This has indeed been demonstrated for the mechanical, catalytic, electrochemical and hydrogen storage properties [10, 11]. In contrast, the cocktail effect on the physical properties has been poorly explored.

Hexagonal close-packed structure is one of the proto-

type structures for HEAs [12]. Although the hexagonal HEAs accounts for only $\sim 1\%$ of the total HEAs, those based on $4d/5d$ elements are known for their proneness to become a superconductor. So far, nearly thirty different superconducting compositions have been found in this family [13–20], and their T_c varies by one order of magnitude up to ~ 8.3 K, as listed in Table 1. Notably, quite a few of these HEAs, such as Mo-Ru-Rh-Pd [13], Mo-Re-Ru-Rh [14], Mo-Re-Ru-Pd-Pt [17], and Mo-W-Re-Ru-Pd [20], have T_c values much higher than those of the corresponding constituent elements. This clearly violates the rule of mixtures and signifies enhanced superconducting pairing induced by the elemental makeup. In this regard, the elucidation of its mechanism not only helps to better understand the cocktail effect and but also may provide clues to achieve a higher T_c . However, to our knowledge, no such study has been reported to date.

Here we address this issue by comparing the experimental T_c , Sommerfeld coefficient γ , and Debye temperature Θ_D values with the compositionally averaged counterparts \bar{T}_c , $\bar{\gamma}$ and $\bar{\Theta}_D$. It is found that, with varying valence electron concentration (VEC), the increase in T_c/\bar{T}_c is concomitant with the decrease in $\Theta_D/\bar{\Theta}_D$. The λ_{ep} dependence of T_c and its affecting factors are examined, and the implications of these results are discussed.

2. PHASE STABILITY

In the hexagonal close-packed lattice, there is only one crystallographic site and hence a solid-solution phase is naturally expected. To confirm this, we calculate the atomic size difference δ and electronegativity difference

*Email address: bliu0201@foxmail.com

†Email address: renzhi@westlake.edu.cn

TABLE I: Physicochemical and physical parameters of the hexagonal HEA superconductors. The data for $\text{Mo}_{0.12}\text{Re}_{0.88}$ and MoReRu alloys are also included for comparison.

Composition	$\delta(\%)$	$\Delta\chi$	VEC	T_c (K)	\bar{T}_c (K)	γ (mJ/molK ²)	$\bar{\gamma}$ (mJ/molK ²)	Θ_D (K)	$\bar{\Theta}_D$ (K)	λ_{ep}	ΔS_{mix}
$\text{Mo}_{50}\text{Ru}_{20}\text{Rh}_{15}\text{Pd}_{15}$ ^[13]	1.763	0.052	7.45	5.0	0.15	—	—	—	—	—	1.237R
$\text{Mo}_{40}\text{Ru}_{40}\text{Rh}_{10}\text{Pd}_{10}$ ^[13]	1.997	0.0354	7.5	3.0	0.32	—	—	—	—	—	1.193R
MoReRuRh ^[14]	1.741	0.142	7.5	2.5	0.58	—	—	—	—	—	1.386R
$(\text{MoReRuRh})_{0.95}\text{Ti}_{0.05}$ ^[14]	2.104	0.187	7.33	3.6	0.57	—	—	—	—	—	1.515R
$(\text{MoReRuRh})_{0.9}\text{Ti}_{0.1}$ ^[14]	2.076	0.224	7.15	4.7	0.69	—	—	—	—	—	1.573R
$\text{Nb}_{10}\text{Mo}_{35}\text{Ru}_{35}\text{Rh}_{10}\text{Pd}_{10}$ ^[15]	2.134	0.181	7.3	5.58	1.09	3.35	4.27	348	424	0.63	1.426R
$\text{Nb}_{15}\text{Mo}_{32.5}\text{Ru}_{32.5}\text{Rh}_{10}\text{Pd}_{10}$ ^[15]	2.105	0.184	7.2	6.19	1.52	3.27	4.58	328	463	0.66	1.476R
$\text{Nb}_{20}\text{Mo}_{30}\text{Ru}_{30}\text{Rh}_{10}\text{Pd}_{10}$ ^[15]	2.076	0.187	7.1	6.10	1.95	2.68	3.88	324	449	0.66	1.505R
$\text{Nb}_5\text{Mo}_{35}\text{Re}_{15}\text{Ru}_{35}\text{Rh}_{10}$ ^[16]	2.074	0.157	7.1	7.54	0.89	3.70	3.21	338	502	0.70	1.40R
$\text{Nb}_5\text{Mo}_{30}\text{Re}_{20}\text{Ru}_{35}\text{Rh}_{10}$ ^[16]	2.048	0.160	7.15	6.69	0.97	3.93	3.22	467	501	0.62	1.431R
$\text{Nb}_5\text{Mo}_{25}\text{Re}_{25}\text{Ru}_{35}\text{Rh}_{10}$ ^[16]	1.997	0.163	7.2	6.51	1.06	4.15	3.24	393	500	0.64	1.441R
$\text{Nb}_5\text{Mo}_{20}\text{Re}_{30}\text{Ru}_{35}\text{Rh}_{10}$ ^[16]	1.985	0.165	7.25	5.46	1.14	3.32	3.76	378	499	0.61	1.431R
$(\text{MoReRu})_{0.916}(\text{PdPt})_{0.084}$ ^[17]	1.698	0.135	7.25	8.17	0.69	3.55	3.11	364	486	0.70	1.353R
$(\text{MoReRu})_{0.834}(\text{PdPt})_{0.166}$ ^[17]	1.636	0.135	7.5	4.91	0.63	3.01	3.57	393	466	0.59	1.481R
$(\text{MoReRu})_{0.75}(\text{PdPt})_{0.25}$ ^[17]	1.570	0.134	7.75	2.22	0.58	2.77	4.04	411	445	0.49	1.56R
$(\text{MoReRu})_{0.66}(\text{PdPt})_{0.34}$ ^[17]	1.498	0.133	8.0	1.64	0.52	2.79	4.55	398	421	0.47	1.60R
MoReRuRhPt ^[18]	1.57	0.140	8.0	0.82	0.48	—	—	—	—	—	1.61R
MoReRuIrPt ^[18]	1.47	0.130	8.0	1.06	0.48	—	—	—	—	—	1.61R
MoReRuRhPd ^[18]	1.20	0.130	8.0	1.38	0.48	—	—	—	—	—	1.61R
MoReRuIrPd ^[18]	1.10	0.117	8.0	1.61	0.48	—	—	—	—	—	1.61R
NbMoReRuRhPt ^{[18]a}	2.42	0.246	7.5	2.95	1.88	—	—	—	—	—	1.79R
NbMoReRuIrPt ^{[18]a}	2.32	0.236	7.5	2.84	1.88	—	—	—	—	—	1.79R
$\text{Ru}_{0.35}\text{Os}_{0.35}\text{Mo}_{0.1}\text{W}_{0.1}\text{Zr}_{0.1}$ ^[19]	4.26	0.278	7.2	2.90	0.50	2.42	2.63	357	504	0.52	1.43R
$\text{Mo}_{35}\text{W}_{10}\text{Re}_{20}\text{Ru}_{30}\text{Pd}_5$ ^[20]	1.84	0.133	7.0	8.32	0.51	3.29	2.85	277	490	0.79	1.43R
MoReRu ^[14]	1.84	0.133	7.0	9.25	0.74	4.23	2.64	339	507	0.76	1.10R
$\text{Mo}_{0.12}\text{Re}_{0.88}$ ^[31]	—	—	6.88	7.45	1.50	3.80	2.41	403	452	0.66	—

^aSample contains a secondary hexagonal phase.

$\Delta\chi$ according to the following equations [21, 22],

$$\delta = \sqrt{\sum_{i=1}^n c_i (1 - r_i / \sum_{i=1}^n c_i r_i)^2}, \quad (1)$$

and

$$\Delta\chi = \sqrt{\sum_{i=1}^n c_i (\chi_i - \sum_{i=1}^n c_i \chi_i)^2}, \quad (2)$$

where n is the number of the constituent elements, and c_i , r_i and χ_i are the molar fraction, atomic radius and electronegativity for the i th constituent element, respectively (variables are the same hereafter). The calculated results are listed in Table I, and δ as well as $\Delta\chi$ are plotted as a

function of VEC in Figs. 1(a) and (b), respectively. Here VEC is given as

$$\text{VEC} = \sum_{i=1}^n c_i (\text{VEC})_i, \quad (3)$$

where $(\text{VEC})_i$ is the valence electron concentration for the i th constituent element. The superconducting hexagonal HEAs exist over a wide range of $7.0 \leq \text{VEC} \leq 8.0$, yet their δ and $\Delta\chi$ fall in the narrow windows of 1.1–3.5% and 0.04–0.25, respectively. Note that the δ values are well below the threshold of 6.6% for the formation of single-phase HEAs. Fig. 1(c) shows the δ plotted as a function of $\Delta\chi$, together with data of hexagonal rare earth HEAs, intermetallic compounds and metallic glasses [23–25] for comparison. As expected, the data of

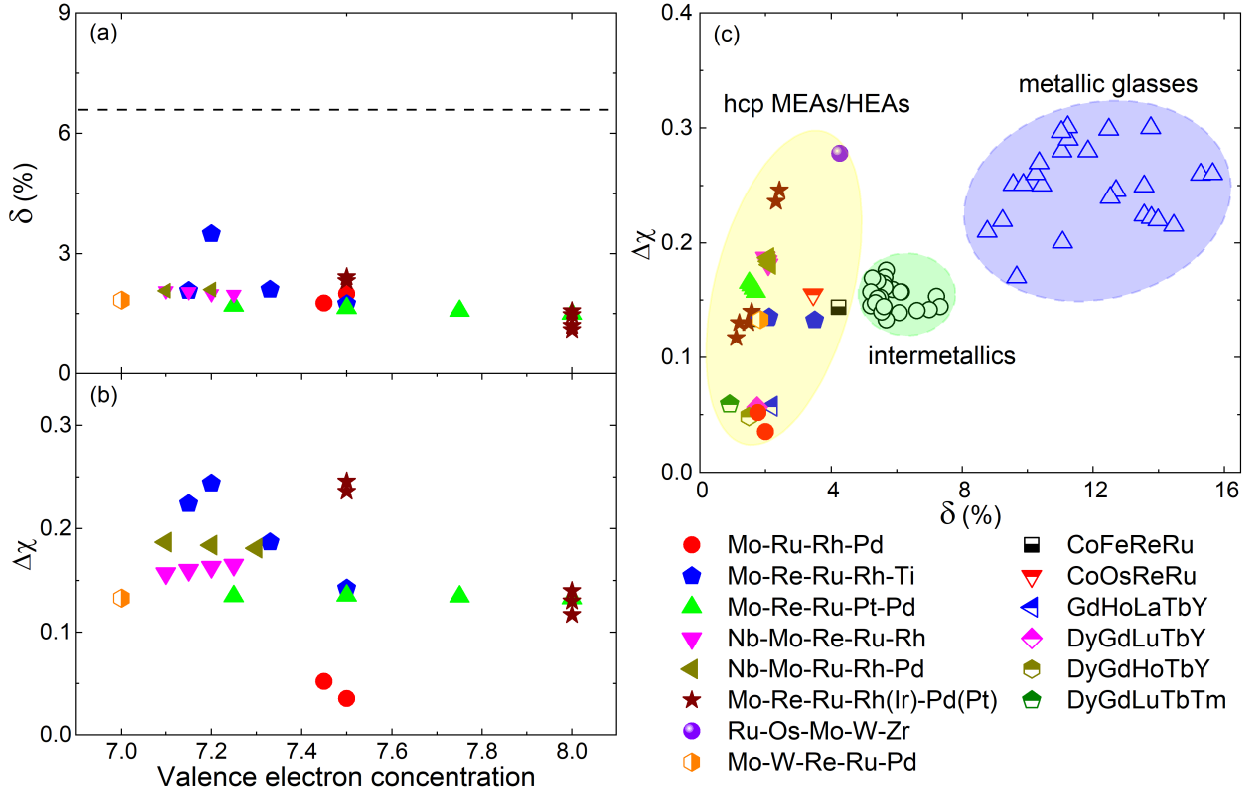


FIG. 1: (a, b) VEC dependencies of δ and $\Delta\chi$, respectively, for the hexagonal HEA superconductors. In panel (a), the horizontal dashed line denotes the threshold for the formation of single-phase HEAs. (c) δ versus $\Delta\chi$ plot of the hexagonal compositionally complex alloy superconductors. The data for rare-earth hexagonal HEAs, typical intermetallics, and metallic glasses are also included for comparison. The regions corresponding to different phases are highlighted in different colors.

all the hexagonal HEAs overlap and are located within the region of $0.9\% \leq \delta \leq 4.2\%$ and $0.035 \leq \Delta\chi \leq 0.278$, which are separated from those of the intermetallic compounds and metallic glasses with larger δ values.

3. COCKTAIL EFFECT ON T_c , γ AND Θ_D

The magnitude of the cocktail effect is elucidated by examining the ratios of T_c/\bar{T}_c , $\gamma/\bar{\gamma}$, and $\Theta_D/\bar{\Theta}_D$, which are plotted as a function of VEC in Figs. 2(a-c), respectively. Following Ref. [26], the compositionally-averaged \bar{T}_c , $\bar{\gamma}$ and $\bar{\Theta}_D$ are calculated using the following equation

$$\bar{X} = \sum_{i=1}^n c_i X_i, \quad (4)$$

where X_i is the parameter value of the i th element (see Table II). The experimental T_c , γ and Θ_D values for the HEAs and individual elements are taken from Refs. [13-20] and Ref. [27, 28], respectively. At VEC = 7.0, the T_c/\bar{T}_c ratio reaches ~ 15 ; this value is much larger than that found in body-centered cubic (bcc) HEA superconductors [29] and indicates a strong cocktail effect. With increasing VEC, the T_c/\bar{T}_c ratio decreases but remains

above 2 up to VEC = 8. As for $\gamma/\bar{\gamma}$ and $\Theta_D/\bar{\Theta}_D$, only the data for the series of Nb-Mo-Ru-Rh-Pd [15], Nb-Mo-Re-Ru-Rh [16], Mo-Re-Ru-Pd-Pt [17] and Mo-W-Re-Ru-Pd [20] HEAs are available. However, since their VECs cover the range of 7.0 to 8.0, the results should be considered as representative. Contrary to those of T_c/\bar{T}_c , the $\gamma/\bar{\gamma}$ ratios are all located near one with the deviation less than 30%, which are smaller than that observed in the bcc HEA superconductor [29]. Instead, the $\Theta_D/\bar{\Theta}_D$ increases with increasing VEC; this is in the opposite trend to that of T_c/\bar{T}_c . At the highest VEC of 8.0, the $\Theta_D/\bar{\Theta}_D$ ratio (~ 0.95) is very close to one, indicating that the rule of mixtures applies well in the case. As the decrease of VEC, however, the $\Theta_D/\bar{\Theta}_D$ ratio decreases by $\sim 40\%$ to 0.57. The concomitant reduction in $\Theta_D/\bar{\Theta}_D$ and enhancement in T_c/\bar{T}_c is reminiscent of the irradiation study on Mo_5Ge_3 [30]. While non-irradiated Mo_5Ge_3 is normal down to 1.6 K, superconductivity below 3.3 K is observed after irradiation and attributed to disorder-induced phonon softening. According to McMillan [31], the λ_{ep} can be expressed as

$$\lambda_{\text{ep}} \equiv \frac{N(0)\langle I^2 \rangle}{M\langle \omega^2 \rangle}, \quad (5)$$

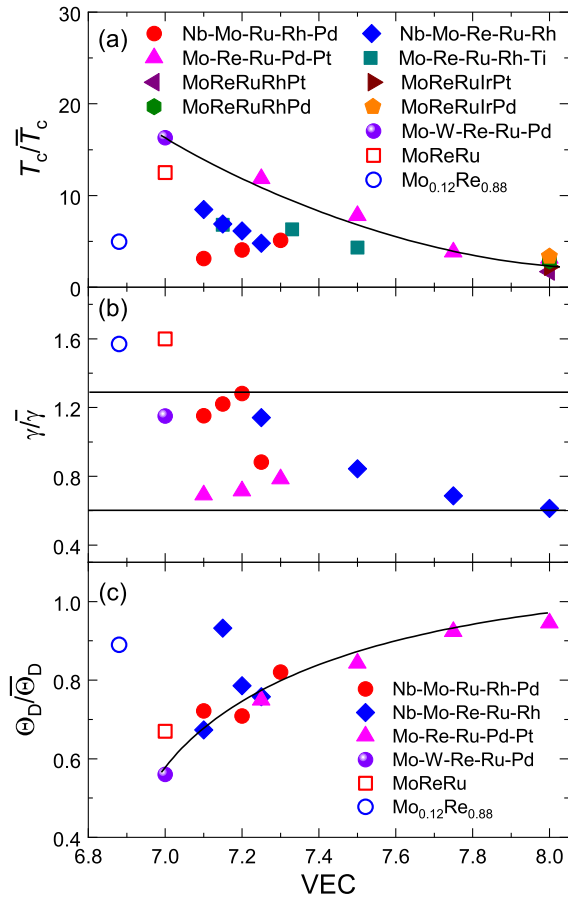


FIG. 2: (a-c) VEC dependencies of T_c/\bar{T}_c , $\gamma/\bar{\gamma}$, and $\Theta_D/\bar{\Theta}_D$, respectively, for the hexagonal HEA superconductors. The data for binary and ternary alloys are also included for comparison and the solid lines are a guide to the eyes.

where $N(0)$ is the bare density of states at the Fermi level, M is the molecular mass, and $\langle I^2 \rangle$ and $\langle \omega^2 \rangle$ are the averaged electron-phonon matrix elements and phonon frequencies, respectively. After irradiation, the $N(0)$ of Mo_5Ge_3 remains almost unaffected while its Θ_D decreases significantly from 377 to 320 K [30]. Since Θ_D is positively correlated with $\langle \omega^2 \rangle$, this leads to a significant increase in λ_{ep} . The high-entropy alloying is similar to radiation in inducing strong atomic disorder and hence phonon softening, which leads to the cocktail of superconductivity properties in the hexagonal HEAs.

To corroborate the presence of cocktail effect, we have also calculated the T_c/\bar{T}_c , $\gamma/\bar{\gamma}$, and $\Theta_D/\bar{\Theta}_D$ of hexagonal $\text{Mo}_{0.12}\text{Re}_{0.88}$ [32] and MoReRu [14] alloys. Compared with the HEAs with (nearly) the same VEC, the T_c/\bar{T}_c ratios are indeed smaller while the $\Theta_D/\bar{\Theta}_D$ ratios are larger for the binary and ternary alloys, indicating a weakened cocktail effect. For dilute alloys, the T_c is typical determined by the component with the highest T_c . However, as all the components approach equimolar ratios, this is no longer case, even for binary alloys. For example,

TABLE II: Parameters of the constituent elements for the hexagonal HEA superconductors. The data are taken from Ref. [27, 28].

Element	VEC	T_c (K)	γ (mJ/molK ²)	Θ_D (K)
Zr	4.0	0.7	3.03	310
Nb	5.0	8.8	8.82	250
Mo	6.0	0.05	2.11	470
W	6.0	0.06	1.21	405
Re	7.0	1.7	2.45	450
Ru	8.0	0.47	3.35	600
Os	8.0	0.71	2.35	500
Rh	9.0	0.09	4.89	478
Ir	9.0	0.1	3.14	420
Pd	10.0	0.1	9.9	299
Pt	10.0	0.1	6.63	221

while Nb has the highest T_c among elements, the T_c of $\text{Nb}_{1-x}\text{V}_x$ and $\text{Ta}_{1-x}\text{V}_x$ alloys with x near 0.5 are lower than those of both the end members [33]. Also in the case of the Nb-Mo-Ru-Rh-Pd HEAs, increasing the Nb content above 15% results in the suppression of T_c [15]. Hence, it is the synergistic effect of all constituent elements rather than individual one that is responsible for the enhancement of T_c compared with the compositional average in hexagonal HEAs.

4. DEPENDENCE OF T_c ON λ_{ep}

In Fig. 3, we plot the T_c data against λ_{ep} and γ for all available cases, in which the λ_{ep} data are taken from Refs. [15-17,19,20]. In contrast with the scattered γ dependence of T_c (see the inset of Fig. 3), the T_c data almost collapse on a single curve as a function of λ_{ep} . At first glance, this "universal" behavior may not be surprising since the λ_{ep} is calculated from T_c and Θ_D using the inverted McMillan formula. Nonetheless, this allows us to estimate the average logarithmic phonon frequency $\langle \omega_{log} \rangle$ using the Allen-Dynes formula [34]

$$T_c = \frac{\langle \omega_{log} \rangle}{1.20} \exp\left[\frac{-1.04(1 + \lambda_{ep})}{\lambda_{ep} - \mu^*(1 + 0.62\lambda_{ep})}\right], \quad (6)$$

where μ^* is the Coulomb repulsion pseudopotential. As can be seen, the λ_{ep} dependence of T_c can indeed be well reproduced with $\langle \omega_{log} \rangle = 235$ K and $\mu^* = 0.11$. Note that the assumption of this constant μ^* is reasonable since it is less important relative to λ_{ep} and lies within the range of 0.1 to 0.13 for transition metals [31]. Meanwhile, the $\langle \omega_{log} \rangle$ value is well comparable with hexagonal Re metal (227 K) [35] and its binary alloys $\text{Nb}_{0.18}\text{Re}_{0.82}$

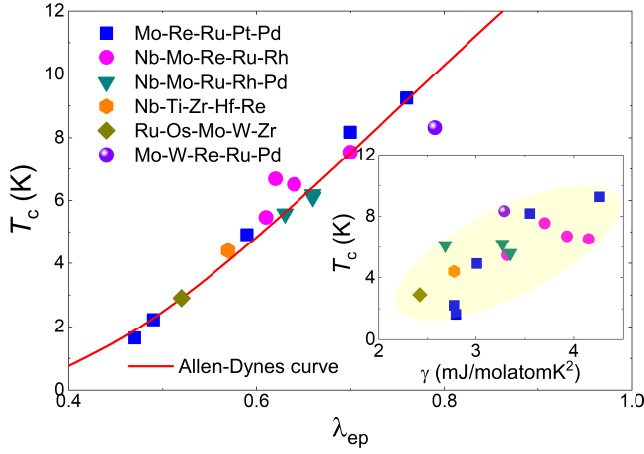


FIG. 3: Available λ_{ep} dependence of T_c for the hexagonal HEA superconductors. The solid line denotes a fit to the data by the Allen-Dynes formula (see text). The inset shows the T_c data plotted as a function of γ . The shaded area is a guide to the eyes.

(264 K) [36], $\text{Mo}_{1-x}\text{Re}_x$ (175-250 K)[37], suggesting that the $\langle\omega_{\log}\rangle$ is not significantly affected by the mixing entropy. The overall results are reminiscent of those found in ternary Tl-Pb-Bi alloys [38], where the $\langle\omega_{\log}\rangle$ is found not to change markedly while the T_c varies appreciably. However, the λ_{ep} of the Tl-Pb-Bi alloys were determined from tunneling experiments [38], which calls for similar studies on the hexagonal HEA superconductors to substantiate the λ_{ep} -dependent T_c behavior.

5. AFFECTING FACTORS ON λ_{ep}

We now discuss the factors that affect λ_{ep} based on equation (5). For the Tl-Pb-Bi alloys [38], it has been shown that the product $N(0)\langle I^2 \rangle$ is not constant throughout the series and the change in λ_{ep} is determined primarily by the variation of $N(0)$. In Fig. 4(a), we plot the λ_{ep} against $\gamma/(1+\lambda_{ep}) \propto N(0)$ for the hexagonal HEA superconductors. One can see that λ_{ep} is at most weakly dependent on $N(0)$, even for the same elemental combination. As noticed by McMillan [31], the $N(0)\langle I^2 \rangle$ remains constant to within 50% for the transition metals V, Nb, Ta, Mo, W although their $N(0)$ and $\langle I^2 \rangle$ vary by nearly one order of magnitude. Such a scenario is more plausible for the hexagonal HEA superconductors considering their constituent elements. Besides, $\langle\omega^2\rangle$ should not change much given the universal $\langle\omega_{\log}\rangle$. Taken together, the λ_{ep} is then expected to scale with the inverse molecular weight of the alloys, M_{alloy} . As illustrated in Fig. 4(b), a linear dependence of λ_{ep} on $1/M_{\text{alloy}}$ is observed for all the series of Mo-Re-Ru-Rh-Pd, Nb-Mo-Re-Ru-Rh, and Nb-Mo-Ru-Rh-Pd HEAs. The slopes for the former two series are comparable but considerably steeper than

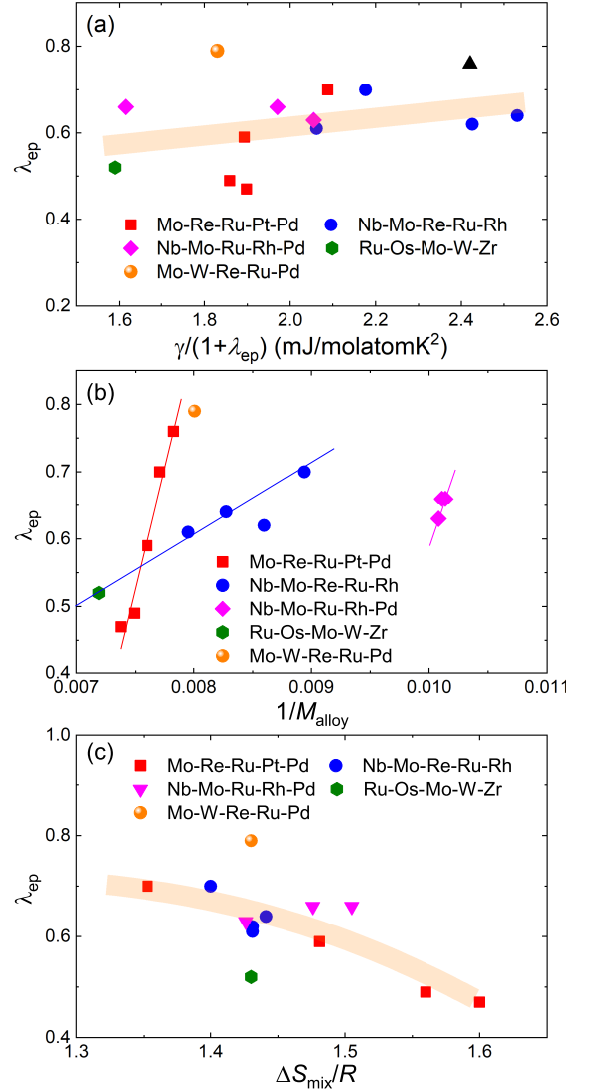


FIG. 4: (a-c) Available λ_{ep} data plotted as functions of $\gamma/(1+\lambda_{ep})$, $1/M_{\text{alloy}}$ and ΔS_{mix} , respectively, for the hexagonal HEA superconductors. The thin and thick lines are guides to the eyes.

that of the latter one. In passing, the data points of the Ru-Os-Mo-W-Zr and Mo-W-Re-Ru-Pd HEAs fall on the gentle and steep slopes, respectively.

A salient feature for the hexagonal HEA superconductors is their large mixing entropy ΔS_{mix} given by the equation

$$\Delta S_{\text{mix}} = -R \sum_{i=1}^n c_i \ln c_i, \quad (7)$$

where R is the gas constant. In this regard, the ΔS_{mix} dependence of λ_{ep} deserves scrutiny and is displayed in Fig. 4(c). With increasing ΔS_{mix} from $\sim 1.43R$ to $\sim 1.60R$, λ_{ep} decreases by more than 30% and the slope becomes steeper, exhibiting a downward curvature. Hence the electron-phonon interaction is reduced progressively as

the atomic disorder gets stronger. In HEA systems, both the electronic and phonon bands are expected to be broadened [39, 40], which smears out the electronic and phononic density states at the Fermi level. Since the T_c of hexagonal HEA superconductors is mainly governed by the λ_{ep} rather than the γ , the broadening of the phonon band should play a more important role than that of the electronic one, consistent with the above result.

We now propose several routes to increase the λ_{ep} in hexagonal HEA superconductors. According to Fig. 4(b), one straightforward way will be to decrease the M by incorporating elements with a lighter atomic mass. Potential candidates include group IIIB elements Sc and Y, both of which can exist in the hexagonal structure. In addition, group IIIA elements Al and Ga, which are known to be useful additives, are also worth trying. On the other hand, increasing the the product $N(0)\langle I^2 \rangle$ provides an alternative approach. This implies an enhancement of the electron-ion interaction and can be achieved by carefully choosing the constituent elements for the HEAs. Especially, the group VIIB element Re appear to be an indispensable component to achieve a large $N(0)\langle I^2 \rangle$. In either case, the ΔS_{mix} should be kept not too large so that its influence on the λ_{ep} is minimized.

6. CONCLUSION

In summary, we have studied the cocktail effect in hexagonal HEA superconductors. It is found that the T_c can be enhanced by one order of magnitude compared to \bar{T}_c , although the $\gamma/\bar{\gamma}$ remains close to one within 30%. Instead, this T_c enhancement is accompanied by the decrease in $\Theta_D/\bar{\Theta}_D$, which underlines the role of phonon softening in the cocktail effect. Furthermore, our analysis indicates that the T_c mainly controlled by the $\langle \omega_{log} \rangle$ and λ_{ep} , and the latter increases linearly with the $1/M_{alloy}$ and is weakened as the increase of ΔS_{mix} . Our results represent a first step toward quantitative understanding the superconducting properties in compositionally complex alloys.

ACKNOWLEDGEMENT

We acknowledge financial support by the foundation of Westlake University, the Yunnan Fundamental Research Projects (202201AU070118, 202401AT070378), the Analysis and Testing Foundation of Kunming University of Science and Technology (2021T20200152).

[1] J. W. Yeh, S. K. Chen, S. J. Lin, J. Y. Gan, T. S. Chin, T. T. Shun, C. H. Tsau, S. Y. Chang. Nanostructured high-entropy alloys with multiple principal elements: novel

alloy design concepts and outcomes. *Adv. Eng. Mater.* **6**, 299 (2004).

[2] Y. F. Ye, Q. Wang, J. Lu, C. T. Liu, and Y. Yang. High-entropy alloy: challenges and prospects. *Mater. Today*, **19**, 349-362 (2016).

[3] D. B. Miracle and O. N. Senkov. A critical review of high entropy alloys and related concepts. *Acta Mater.* **122**, 448 (2017).

[4] E. P. George, D. Raabe, and R. O. Ritchie. High-entropy alloys. *Nat. Rev. Mater.* **4**, 515 (2019)

[5] W. Li, D. Xie, D. Li, Y. Zhang, Y. Gao, and P. K. Liaw. Mechanical behavior of high-entropy alloys. *Prog. Mater. Sci.* **118**, 100777 (2021).

[6] Y. Y. Zhao, H. W. Chen, Z. P. Lu, and T. G. Nieh. Thermal stability and coarsening of coherent particles in a precipitation-hardened $(\text{NiCoFeCr})_{94}\text{Ti}_2\text{Al}_4$ high-entropy alloy. *Acta Mater.* **147**, 184-194 (2018).

[7] Y. Qiu, S. Thomas, M. A. Gibson, H. L. Fraser, and N. Birbilis. Corrosion of high entropy alloys. *npj Mat. Degrad.* **1**, 15 (2017).

[8] V. Chaudhary, R. Chaudhary, R. Banerjee, and R. V. Ramanujan. Accelerated and conventional development of magnetic high entropy alloys. *Mater. Today*, **49**, 231-252 (2021).

[9] F. Von Rohr, M. J. Winiarski, J. Tao, T. Klimczuk, and R. J. Cava. Effect of electron count and chemical complexity in the Ta-Nb-Hf-Zr-Ti high-entropy alloy superconductor. *Proc. Natl. Acad. Sci.* **113**, E7144-E7150 (2016).

[10] E. P. George, W. A. Curtin, and C. C. Tansan. High entropy alloys: A focused review of mechanical properties and deformation mechanisms. *Acta Mater.* **188**, 435-474 (2020).

[11] D. Liu, P. Guo, H. Pan, and R. Wu. Emerging high-entropy compounds for electrochemical energy storage and conversion. *Prog. Mater. Sci.* **145**, 101300 (2024).

[12] M. C. Gao, B. Zhang, S. M. Guo, J. W. Qiao, and J. A. Hawk. High-entropy alloys in hexagonal close-packed structure. *Metall. Mater. Trans. A* **47**, 3322-3332 (2016).

[13] J. G. Lee, Y. J. Park, H. Y. Pyo, J. G. Kim, K. Y. Jee, W. H. Kim, and Y. Jeon. XPS studies of superconducting Mo-Ru-Rh-Pd alloy. *J. Alloys Compd.* **298**, 291-294 (2000).

[14] Y. S. Lee and R. J. Cava. Superconductivity in high and medium entropy alloys based on MoReRu. *Physica. C.* **566**, 1353520 (2019).

[15] B. Liu, J. F. Wu, Y. W. Cui, Q. Q. Zhu, G. R. Xiao, S. Q. Wu, G. H. Cao, and Z. Ren. Superconductivity in hexagonal Nb-Mo-Ru-Rh-Pd high-entropy alloys. *Scripta Mater.* **182**, 109-113 (2020).

[16] B. Liu, J. F. Wu, Y. W. Cui, Q. Q. Zhu, G. R. Xiao, S. Q. Wu, G. H. Cao, and Z. Ren. Structural evolution and superconductivity tuned by valence electron concentration in the Nb-Mo-Re-Ru-Rh high-entropy alloys. *J. Mater. Sci. Technol.* **85**, 11-17 (2021).

[17] Q. Q. Zhu, G. R. Xiao, Y. W. Cui, W. Z. Yang, S. J. Song, G. H. Cao, and Z. Ren. Structural transformation and superconductivity in carbon-added hexagonal high-entropy alloys. *J. Alloys Compd.* **909**, 164700 (2022).

[18] A. J. Browne, D. P. Strong, and R. J. Cava. Phase stability and possible superconductivity of new $4d$ and $5d$ transition metal high-entropy alloys. *J. Solid State Chem.* **321**, 123881 (2023).

[19] K. Motla, S. Jangid, P. K. Meena, R. K. Kushwaha, and

- R. P. Singh. Superconducting properties of new hexagonal and noncentrosymmetric cubic high entropy alloys. *Supercond. Sci. Tech.* **36**, 115024 (2023).
- [20] X. Xu, W. Z. Yang, H. Y. Song, J. S. Wang, L. Yu, Z. Ren, and B. Liu. Structural sequence and superconductivity in high-entropy Mo-W-Re-Ru-Pd alloys. *Scripta Mater.* **243**, 115986 (2024).
- [21] Y. Zhang, Y. J. Zhou, J. P. Lin, G. L. Chen, and P. K. Liaw. Solid-solution phase formation rules for multi-component alloys. *Adv. Eng. Mater.* **10**, 534-538 (2008).
- [22] X. Chang, M. Zeng, K. Liu, and L. Fu. Phase engineering of high-entropy alloys. *Adv. Mater.* **32**, 1907226 (2020).
- [23] S. Marik, K. Motla, M. Varghese, K. P. Sajilesh, D. Singh, Y. Breard, P. Boullay, and R. P. Singh. Superconductivity in a new hexagonal high-entropy alloy. *Phys. Rev. Mater.* **3**, 060602 (2019).
- [24] J. W. Qiao, M. L. Bao, Y. J. Zhao, H. J. Yang, Y. C. Wu, Y. Zhang, J. A. Hawk and M. C. Gao. Rare-earth high entropy alloys with hexagonal close-packed structure. *J. Appl. Phys.* **124**, 195101 (2018).
- [25] M. C. Gao and D. E. Alman. Searching for next single-phase high-entropy alloy compositions. *Entropy* **15**, 4504-4519 (2013).
- [26] P. Kozelj, S. Vrtnik, A. Jelen, S. Jazbec, Z. Jaglicic, S. Maiti, M. Feuerbacher, W. Steurer, and J. Dolinsek. Discovery of a Superconducting High-Entropy Alloy. *Phys. Rev. Lett.* **113**, 107001 (2014).
- [27] B. T. Matthias. Chapter V Superconductivity in the periodic system. *Prog. Low Temp. Phys.* **2**, 138 (1957).
- [28] E. S. R. Gopal. Specific heats at low temperatures. Plenum Press, New York (1966).
- [29] J. Kitagawa, S. Hamamoto, and N. Ishizu. Cutting edge of high-entropy alloy superconductors from the perspective of materials research. *Metals* **10**, 1078 (2020).
- [30] A. K. Ghosh and R. Caton. Heat capacity measurements on irradiated and non-irradiated Mo_3Ge and Mo_5Ge_3 . *Solid State Commun.* **44**, 1083-1085 (1982).
- [31] W. L. McMillan. Transition Temperature of Strongly Coupled Superconductors. *Phys. Rev.* **167**, 331 (1968).
- [32] T. Shang, D. J. Gawryluk, J. A. T. Verezhak, E. Pomjakushina, M. Shi, M. Medarde, J. Mesot, and T. Shiroka. Structure and superconductivity in binary $\text{Re}_{1-x}\text{Mo}_x$ alloys. *Phys. Rev. Mater.* **3**, 024801 (2019).
- [33] J. M. Corsan and A. J. Cook. Specific Heat and Superconductivity of Binary Alloys Containing V, Nb, and Ta. *Phys. Stat. Sol.* **40**, 657 (1970).
- [34] P. B. Allen and C. R. Dynes. Superconductivity and phonon softening: II. Lead alloys. *Phys. Rev. B* **11**, 1895 (1975).
- [35] Y. L. Shitikov, N. A. Tulina, and M. G. Zemlyanov. Special features of lattice dynamics and electron-phonon interaction in Re. *Phys. Status Sol. (b)*, **133**, 469-474 (1986).
- [36] A. B. Karki, Y. M. Xiong, N. Haldolaarachchige, S. Stadler, I. Vekhter, P. W. Adams, D. P. Young, W. A. Phelan, and J. Y. Chan. Physical properties of the noncentrosymmetric superconductor $\text{Nb}_{0.18}\text{Re}_{0.82}$. *Phys. Rev. B* **83**(14), 144525 (2011).
- [37] D. P. Shum, A. Bevolo, J. L. Staudenmann, and E. L. Wolf. Enhanced Superconductivity by Electron Renormalization of a Directly Observed Brout-Visscher Local Phonon: Re in $\text{Mo}_{1-x}\text{Re}_x$. *Phys. Rev. Lett.* **57**, 2987 (1986).
- [38] R. C. Dynes and J. M. Rowell. Influence of electrons-per-atom ratio and phonon frequencies on the superconducting transition temperature of lead alloys. *Phys. Rev. B* **11**, 1884 (1975).
- [39] S. Gutowska, A. Kawala, and B. Wiendlocha. Superconductivity near the Mott-Ioffe-Regel limit in the high-entropy alloy superconductor $(\text{ScZrNb})_{1-x}(\text{RhPd})_x$ with a CsCl-type lattice. *Phys. Rev. B* **108**, 064507 (2023).
- [40] J. Kitagawa, K. Hoshi, Y. Kawasaki, R. Kaga, Y. Mizuguchi, and T. Nishizaki. Superconductivity and hardness of the equiatomic high-entropy alloy Hf-MoNbTiZr . *J. Alloys Compd.* **924**, 166473 (2022).